FCN: Fusing Exponential and Linear Cross Network for Click-Through Rate Prediction

Honghao Li
salmon1802li@gmail.com
Anhui University
Hefei, Anhui Province, China

Yiwen Zhang*
zhangyiwen@ahu.edu.cn
Anhui University
Hefei, Anhui Province, China

Yi Zhang
zhangyi.ahu@gmail.com
Anhui University
Hefei, Anhui Province, China

Hanwei Li
lihanwei@stu.ahu.edu.cn
Anhui University
Hefei, Anhui Province, China

Lei Sang
sanglei@ahu.edu.cn
Anhui University
Hefei, Anhui Province, China

Jieming Zhu
jiemingzhu@ieee.org
Huawei Noah's Ark Lab
Shenzhen, Guangdong Province
China

Abstract

As an important modeling paradigm in click-through rate (CTR) prediction, the Deep & Cross Network and its derivative models have gained widespread recognition, primarily due to their success in trade-off computational cost and performance. However, this paradigm typically depends on deep neural network (DNN) to implicitly learn high-order feature interactions, without explicitly modeling extremely high-order interactions due to concerns about model complexity. To address this limitation, we propose a novel model for CTR prediction, called the Fusing Cross Network (FCN), which consists of two sub-networks: the Exponential Cross Network (ECN) and the Linear Cross Network (LCN). Specifically, ECN explicitly captures extremely high-order feature interactions whose order increases exponentially with network depth, while LCN captures low-order feature interactions with linearly increasing order. By integrating these two sub-networks, FCN is able to explicitly model a broad spectrum of feature interactions, thereby eliminating the need to rely on implicit modeling by DNN. Moreover, we introduce a low-cost aggregation method that reduces the number of parameters by 50% and inference latency by 23%. Meanwhile, we propose a simple yet effective loss function, Tri-BCE, which provides tailored supervision signals for each sub-network. We evaluate the effectiveness and efficiency of FCN on six public benchmark datasets and 16 baselines. Furthermore, we verify the effectiveness of the FCN on a real-world business dataset spanning seven days. The code, running logs, and detailed hyperparameter configurations are publicly available at https://github.com/salmon1802/FCN.

CCS Concepts

• **Information systems → Recommender systems**.

*Corresponding author

Keywords

Feature Interaction, Cross Network, Recommender Systems, CTR Prediction

1 Introduction

Click-through rate (CTR) prediction is an essential part of industrial recommender systems and online advertising [33, 44, 54, 56]. It uses heterogeneous features as model inputs, such as user profiles, item attributes, and context [14, 55]. These features undergo interaction modeling to predict the probability that a user will click on an item, thereby providing a better user experience and increasing the profitability of the recommender system [2, 7, 43].

As a representative feature interaction-based CTR modeling paradigm, Deep & Cross Network (DCN) [42, 43] achieves a favorable trade-off between computational cost and model performance, attracting considerable attention from CTR researchers [4, 19, 34, 36]. As its name suggests, DCN is a "deep and cross" network rather than a "deep cross" network, as it consists of both a deep neural network (DNN) and a cross network (CrossNet). In this architecture, the DNN is responsible for modeling implicit high-order feature interactions, while the CrossNet explicitly captures low-order feature interactions, typically only up to the third or fourth order [19, 56]. Nevertheless, several studies [20, 39, 55] indicate that high-order feature interactions are beneficial for model performance, but modeling extremely high-order interactions remains challenging due to gradient [8], rank [6], and noise [20] issues. Furthermore, with the establishment of open-source benchmarks [54, 56], researchers observe that CTR models appear to encounter a performance bottleneck: when well-tuned hyperparameters are used, the performance gap among models becomes small. For example, as shown in Figure 1, the AUC of most CTR models ranges from 81.35 to 81.50. Moreover, some studies demonstrate that DNN, in practice, struggle to learn multiplicative feature interactions within a limited representation space [29, 43] and often occupy a large proportion of
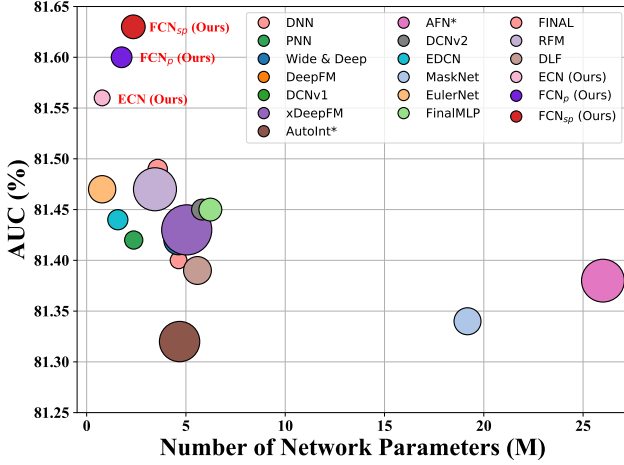
Figure 1: Comparison among ECN, FCN, and other models in terms of network parameter number, AUC, and running time on Criteo dataset. The graphic area represents the running time per epoch for each model (a larger area indicates a longer time, and vice versa).

network parameters in large-scale production data [43]. Taken together, these findings suggest a promising direction for overcoming the performance bottleneck: *Can we remove the dependence on DNN in CTR modeling paradigm and instead employ a truly "deep cross" network to capture extremely high-order explicit feature interactions?*

To answer this question, we revisit the DCNv2 model [43] and decompose the modeling process of CrossNetv2 into an aggregation step and an interaction step. Furthermore, we conduct both theoretical and empirical analyses of these two steps. Our results reveal that approximately half of the weight parameters in the aggregation step are relatively redundant, while in the interaction step, the model only considers the interactions between the aggregated feature information and first-order features, which leads to feature interactions with an inefficient linear growth.

To address these limitations and achieve a truly "deep cross" network, this paper proposes a novel explicit feature interactions model for CTR prediction, called the **Fusing Cross Network (FCN)**. Specifically, FCN consists of two complementary sub-networks: (1) the **Exponential Cross Network (ECN)**, which aims to capture exponentially growing extremely high-order feature interactions; and (2) the **Linear Cross Network (LCN)**, which focuses on capturing linearly growing low-order feature interactions. Besides, we introduce a **Low-cost Aggregation** method to alleviate computational redundancy in the aggregation step, reducing the number of parameters by nearly 50% and inference latency by about 23%, with negligible impact on model performance. Moreover, we propose a simple yet effective loss function, named **Tri-BCE**, which provides appropriate supervision signals for different sub-networks. The core contributions of this paper are summarized as follows:

- To the best of our knowledge, this is the first work to achieve surprising performance using only explicit feature interaction modeling without integrating DNN.

- We propose a novel network, called ECN, which captures extremely high-order explicit feature interactions whose order increases exponentially with network depth. To reduce computational redundancy, we introduce a low-cost aggregation method. Furthermore, we design a simple yet effective loss function, Tri-BCE, to provide tailored supervision signals for different sub-networks.

- We propose a novel CTR model and design two fusion architectures, FCN_p and FCN_{sp}, which can adapt to various data distributions by capturing feature interactions of suitable orders.

- Comprehensive experiments on six benchmark datasets and 16 baselines demonstrate the effectiveness and efficiency of FCN. Based on our experimental results, our models achieve 1st rankings on multiple CTR prediction benchmarks.

2 Related Work

Effectively capturing feature interactions has always been one of the key methods for improving CTR prediction, thus receiving extensive research attention [36, 39, 55]. Traditional methods include LR [30], which captures first-order feature interactions, and FM [28] and its derivatives [23, 35, 48], which capture second-order feature interactions. With the rise of deep learning, several models attempt to use DNN to capture high-order feature interactions (e.g., PNN [26], Wide & Deep [3], DeepFM [7], DCNv1 [42], DCNv2 [43], SimCEN [15], RFM [37], and DIN [52]), achieving better performance. Among these, the DCN series models are widely recognized for their effective trade-off between efficiency and performance, gaining significant attention from both academia and industry [2, 19, 39, 42, 43, 49, 51]. Most subsequent deep CTR models follow the paradigm established by DCN, integrating explicit and implicit feature interactions.

Explicit feature interactions are often modeled directly through hierarchical structures, such as the Cross Layer in the DCN [42], the Graph Layer in FiGNN [18], and the Interacting Layer in AutoInt [34]. These methods ensure partial interpretability while allowing the capture of finite-order feature interactions. On the other hand, some studies attempt to integrate implicit feature interactions by designing different structures. These structures mainly include stacked structures [26, 27, 49], parallel structures [14, 39, 55], and alternate structures [15, 55]. The introduction of these structures not only enhances the expressive power of the models but also captures high-order feature interactions through DNN, leading to significant performance improvements in practical applications.

However, as the performance of explicit feature interactions is generally weaker than that of implicit feature interactions [22], several models attempt to abandon standalone explicit interaction methods and instead integrate multiplicative operations into DNN. MaskNet [45] introduces multiplicative operations block by block, while GateNet [10], PEPNet [1], FINAL [55], and QNN-α [17] introduce them layer by layer to achieve higher performance. Moreover, implicit large language model augmentation methods [32, 46, 47] have also contributed to advancements in the CTR prediction task. Nevertheless, most models struggle to explicitly capture extremely high-order feature interactions and fail to provide appropriate supervision signals for different sub-networks. This paper aims to address these limitations through our proposed methods.

3 Preliminary

3.1 CTR Prediction

It is typically considered a binary classification task that utilizes user profiles, item attributes, and context as features to predict the probability of a user clicking on an item [34, 56]. The composition of these three types of features is as follows:

- *User profiles* (x_U): age, gender, occupation, etc.
- *Item attributes* (x_I): brand, price, category, etc.
- *Context* (x_C): timestamp, device, position, etc.

Further, we can define a CTR input sample in the tuple data format: $X = \{x_U, x_I, x_C\}$. $y \in \{0, 1\}$ is an true label for user click behavior:

$$y = \begin{cases} 1, & \text{user has clicked item,} \\ 0, & \text{otherwise,} \end{cases} \tag{1}$$

where $y = 1$ represents a positive sample and $y = 0$ represents a negative sample. A CTR prediction model aims to predict y and rank items based on the predicted probabilities $\hat{y}$.

3.2 Embedding Layer

The input feature X of the CTR prediction task, which is multi-field categorical data and is represented using one-hot encoding. Most CTR prediction models [14, 31, 34] utilize an embedding layer to transform them into low-dimensional dense vectors: $e_i = E_i x_i$, where $E_i \in \mathbb{R}^{d \times s_i}$ and s_i separately indicate the feature field embedding matrix and the vocabulary size for the i-th field, d represents the embedding dimension. Finally, we concatenate these dense vectors to obtain the input $x_1 = [e_{(1,1)}, e_{(1,2)}, \cdots, e_{(1,f)}] \in \mathbb{R}^D$ of the feature interaction layer, where $D = \sum_{i=1}^{f} d$, f denotes the number of fields, $e_{(l,i)} \in \mathbb{R}^d$ denotes the l-th order feature of the i-th feature field, and x_1 denotes the original **first-order features.**[1]

4 Revisiting Feature Interactions in DCNv2

DCNv2 [43] is a widely recognized modeling paradigm in the CTR prediction task. To better understand how DCNv2 works, we conduct an in-depth analysis of its mechanisms.

4.1 Implicit Feature Interaction

It aims to automatically learn complex non-manually defined data patterns and high-order feature interactions using DNN [19, 43]. Formally, for a given input feature x^1, the implicit feature interaction process can be expressed as:

$$h_{k+1} = \sigma(W_k h_k + b_k), \quad k = 1, 2, \ldots, K, \tag{2}$$

where $h_1 = x_1$, h_{k+1} denotes the output of the k-th layer, and σ represents the activation function. Compared to explicit feature interaction, implicit feature interaction does not have a concrete interaction form, but it learns the inherent data distribution [19, 43]. It is highly efficient and performs well [56], but it has difficulty learning multiplicative feature interactions [29, 43].

4.2 Explicit Feature Interaction

*4.2.1 **Re-Analysis for CrossNetv2.*** Explicit feature interaction seeks to directly capture the combinations and relationships among input features by employing predefined multiplicative interaction functions with controllable order. A popular method for explicit feature interaction is **CrossNetv2** [43], which is described as follows:

$$x_{l+1} = x_1 \odot (W_l x_l + b_l) + x_l, \quad l = 1, 2, \ldots, L, \tag{3}$$

where $x_l \in \mathbb{R}^D$ denotes the features of l-th order, $\odot$ is the Hadamard Product, and $W_l \in \mathbb{R}^{D \times D}$ and $b_l \in \mathbb{R}^D$ are the learnable weight matrix and bias vector at l-th layer. This method uses the Hadamard Product to interact feature x_l with **anchor features**[2] x_1 to generate the $(l+1)$-th order feature x_{l+1}. To more intuitively illustrate how Eq. (3) performs feature interaction, we decompose it into aggregation and interaction steps, and rewrite it as follows (ignoring the bias and residual terms):

$$\text{Aggregation: } c_l = W_l x_l = \begin{bmatrix} W_{(l,1,1)} & \cdots & W_{(l,1,f)} \\ \vdots & \ddots & \vdots \\ W_{(l,f,1)} & \cdots & W_{(l,f,f)} \end{bmatrix} \begin{bmatrix} e_{(l,1)} \\ e_{(l,2)} \\ \vdots \\ e_{(l,f)} \end{bmatrix}$$

$$= \left[\sum_{i=1}^{f} W_{(l,1,i)} e_{(l,i)}, \sum_{i=1}^{f} W_{(l,2,i)} e_{(l,i)}, \ldots, \sum_{i=1}^{f} W_{(l,f,i)} e_{(l,i)} \right]^\top, \tag{4}$$

$$\text{Interaction: } x_{l+1} = x_1 \odot c_l = \begin{bmatrix} e_{(1,1)} \odot \sum_{i=1}^{f} W_{(l,1,i)} e_{(l,i)} \\ e_{(1,2)} \odot \sum_{i=1}^{f} W_{(l,2,i)} e_{(l,i)} \\ \vdots \\ e_{(1,f)} \odot \sum_{i=1}^{f} W_{(l,f,i)} e_{(l,i)} \end{bmatrix} \tag{5}$$

where $W_{(l,i,j)} \in \mathbb{R}^{d \times d}$ represents the importance of interaction between the i-th and j-th feature fields at the l-th layer, and c_l aggregates all l-order feature at the l-th layer. From Eqs. (4) and (5), we observe that the seemingly simple operation $x_1 \odot c_l$ actually accomplishes two steps:

- **Aggregation Step**: It aggregates information from all feature fields for each feature field.
- **Interaction Step**: It interacts the aggregated information with *first-order features* to generate higher-order features.

This simple two-step approach implements explicit feature interactions with linear growth. DCNv2 combines this approach with implicit feature interactions, thereby further enhancing the model's ability to capture complex feature relationships. However, CrossNetv2 encounters two issues that require further investigation.

*4.2.2 **Computational Redundancy in the Aggregation Step.*** To investigate whether the weight matrix W_l in the aggregation step fully utilizes the parameter space, we perform singular value decomposition (SVD) [38] and analyze the distribution of singular values to determine whether computational redundancy exists. Specifically, for a parameter matrix W, we perform SVD as $W = U\Sigma V^\top$,

---

[1]In this paper, to ensure that the number of network layers aligns with the order of feature interactions, we take the input x_1 as the first-order feature.

[2]To more intuitively illustrate the similarities and differences between linear and exponential feature interactions, we refer to the feature that is not aggregated by the weight matrix as the anchor feature.
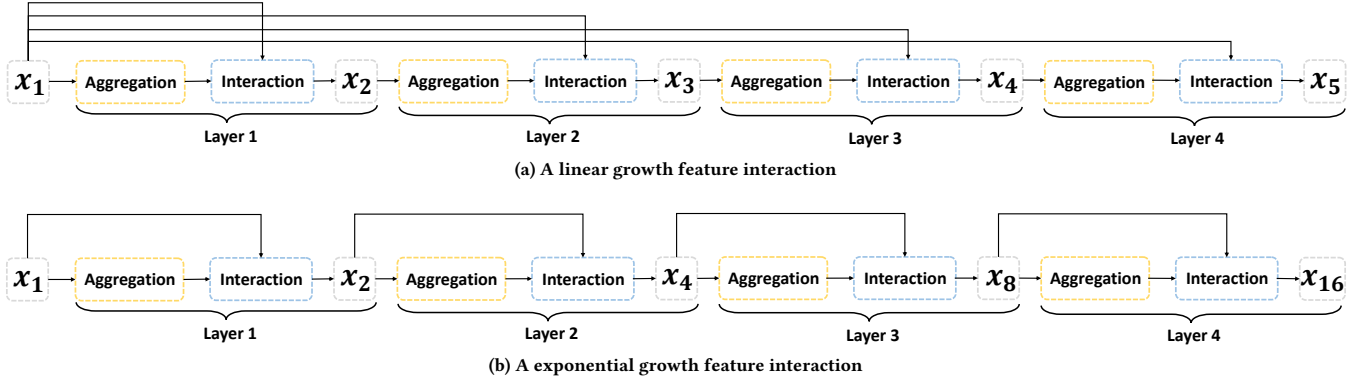
(a) A linear growth feature interaction

(b) A exponential growth feature interaction

Figure 2: A comparison between feature interaction methods with linear and exponential growth.
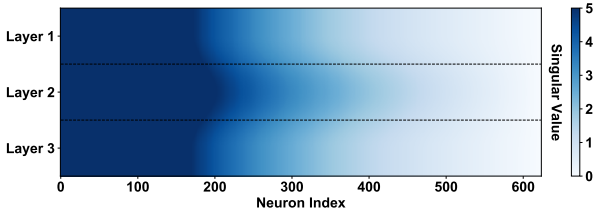

Figure 3: The singular value distribution [38] of the weight matrix $\mathbf{W}_l$ in each layer of CrossNetv2 on Criteo dataset.

where Σ denotes the incrementally ordered singular value distribution of $\mathbf{W}$. A smaller singular value in a particular dimension indicates lower utilization and more severe redundancy [9, 12]. The experimental results are presented in Figure 3. We observe that nearly half of the singular values of the weight matrix $\mathbf{W}_l$ in CrossNetv2 are relatively small, indicating redundancy in the parameter space. This finding motivates us to explore a more lightweight method for measuring the importance of interactions between feature fields.

*4.2.3   **Inefficient Feature Interaction in the Interaction Step**.* To provide a more intuitive explanation of why CrossNetv2 implements feature interactions with linear growth, we visualize its interaction process in Figure 2 (a). Consistent with Eq. (5), each layer of CrossNetv2 first aggregates information from all feature fields and then interacts with x_1 to generate the x_{l+1} feature. This method, which fixes the interaction to x_1 after aggregation, limits the efficiency of feature interactions.

To address the inefficiency in feature interaction modeling, a simple yet effective method is to replace the anchor feature x_1 with $x_{2^{l-1}}$, as illustrated in Figure 2 (b). By interacting the aggregated information with $x_{2^{l-1}}$ at each layer, we achieve exponentially growing feature interactions. As shown in Figure 2, when both methods are stacked for four layers, the linear feature interaction can only model up to x_5, whereas the exponential feature interaction can model up to x_{16}.

5   Methodology

Based on the findings presented in Section 4, we propose the FCN model, shown in Figure 4, which integrates different explicit feature interaction sub-networks: LCN and ECN, enabling it to simultaneously explicitly capture both low-order and high-order feature interactions.

5.1   Fusing Cross Network

Previous deep CTR models [7, 19, 39, 43] typically employ explicit interaction methods to capture low-order feature interactions and rely on DNN to implicitly capture high-order feature interactions. However, the former is limited to capturing low-order interactions due to complexity constraints and generally exhibits lower performance [22, 55, 56], while the latter struggles to learn multiplicative feature interactions within a limited representation space [29, 43]. Therefore, we aim to achieve a truly "deep cross" network that captures explicit high-order feature interactions, thereby eliminating the dependence of CTR models on DNN.

*5.1.1   **Low-cost Aggregation (LCA)**.* As presented in Section 4.2.2, nearly half of the parameter space of the weight matrix $\mathbf{W}_l$ in the cross network remains underutilized. Therefore, we directly reduce the size of the weight matrix by half and introduce a low-cost affine transformation to maintain consistency with the original output dimension. For clarity, we provide the visualization shown in Figure 5. Formally, we define this process as follows:

$$\text{LCA}\,(x_l) = \left[c_{(l,1)} \| c'_{(l,1)}, c_{(l,2)} \| c'_{(l,2)}, \cdots, c_{(l,f)} \| c'_{(l,f)} \right],$$

$$c_{(l,i)} = \sum_{j=1}^{f} \left(W_{(l,i,j)} e_{(l,j)} + b_{(l,i,j)} \right),\quad l = 1, 2, \ldots, L, \qquad (6)$$

$$c'_{(l,i)} = \gamma_{(l,i)} \odot c_{(l,i)} + \beta_{(l,i)},$$

where $W_{(l,i,j)} \in \mathbb{R}^{\frac{d}{2} \times d}$ denotes the importance of interaction between the i-th and j-th feature fields at the l-th layer, $c_{(l,i)}$ is the aggregation vector of all features fields for the i-th feature field, $\gamma_{(l,i)}, \beta_{(l,i)} \in \mathbb{R}^{\frac{d}{2}}$ are the affine parameters for the i-th feature field, and $\|$ denotes the concatenation operation. LCA employs low-cost affine transformations to halve the parameter space required for
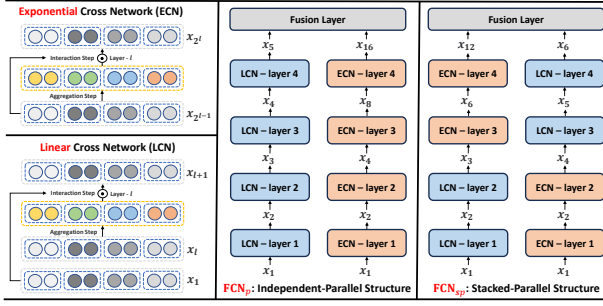
Figure 4: An example of the modeling processes of FCN_p and FCN_{sp}.
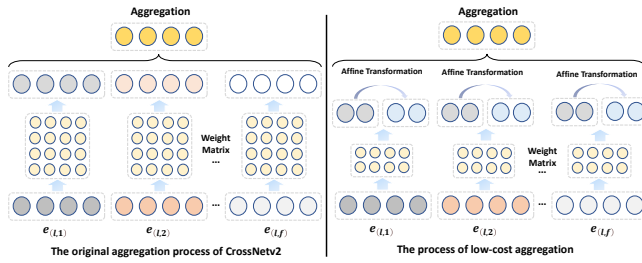

Figure 5: A comparison between the original aggregation process and the low-cost aggregation process.

the aggregation step, thereby enhancing the efficiency of feature information aggregation.

5.1.2 **Linear Cross Network (LCN)**. LCN adopts the same idea as CrossNetv2. It is utilized to capture low-order explicit feature interactions with linear growth. Its recursive formulation is:

$$x_{l+1} = x_1 \odot \text{LCA}(x_l) + x_l, \quad l = 1, 2, \dots, L, \quad (7)$$

where the anchor features are x_1, and the aggregated features $\text{LCA}(x_l)$ interact with x_1 to generate the $(l+1)$-th order feature.

5.1.3 **Exponential Cross Network (ECN)**. As the core idea of FCN, it is used to capture *extremely high-order* explicit feature interactions with exponential growth. Its recursive formula is:

$$x_{2^l} = x_{2^{l-1}} \odot \text{LCA}(x_{2^{l-1}}) + x_{2^{l-1}}, \quad l = 1, 2, \dots, L, \quad (8)$$

where $x_{2^l} \in \mathbb{R}^D$ represents the 2^l-th order feature. Unlike LCN, ECN modifies the anchor features from x_1 to $x_{2^{l-1}}$, thereby achieving high-order feature interactions within a limited number of layers. To more clearly illustrate the similarities and differences between LCN and ECN, we provide pseudocode in Figure 6. Combining the results in Figure 1, we observe that ECN achieves SOTA performance by modifying only a single variable based on LCN.

5.1.4 **Fusing LCN and ECN**. Most previous CTR models [22, 43, 55] attempt to model explicit and implicit feature interactions, which essentially means capturing both low-order and high-order feature interactions. Our FCN achieves this by fusing LCN and ECN, avoiding the use of DNN. Specifically, we propose two fusion architectures:

```
# Pseudocode for the implementation of LCN and ECN.
def cross_layer(self, x, x_anchor, i):
    c = self.LCA(x)   # Aggregation.
    return x_anchor * c + x   # Interaction.
def lcn_forward(self, x, x_1):   # Pseudocode of LCN.
    for i in range(self.lcn_num_layers):
        x = self.cross_layer(x, x_1, i)
    return x
def ecn_forward(self, x):   # Pseudocode of ECN.
    for i in range(self.ecn_num_layers):
        x = self.cross_layer(x, x, i)
    return x
```

Figure 6: Pseudocode for LCN and ECN.

- **FCN_p: Independent-Parallel architecture**: It allows LCN and ECN to process input features separately.
- **FCN_{sp}: Stacked-Parallel architecture**: It sequentially stacks one network on top of the other.

These two fusion architectures are illustrated in Figure 4. We observe that FCN_p captures the features $[x_1, x_2, x_3, x_4, x_5, x_8, x_{16}]$, while FCN_{sp} captures the features $[x_1, x_2, x_3, x_4, x_5, x_6, x_{12}]$. This indicates that the two architectures focus on different orders of feature interaction modeling. In practice, the choice of fusion architecture can be adjusted according to the order of feature interactions required by the data distribution.

Finally, we use a simple linear transformation to convert the output representation of the FCN into the final prediction[3]. Taking FCN_p as an example, the fusion layer is formalized as follows:

$$\hat{y} = \text{Mean}(\hat{y}_{exp}, \hat{y}_{lin}),$$
$$\hat{y}_{exp} = \sigma(\mathbf{W}_{exp} x_{2^L} + b_{exp}), \quad \hat{y}_{lin} = \sigma(\mathbf{W}_{lin} x_{L+1} + b_{lin}), \quad (9)$$

where $\mathbf{W}_{exp}$ and $\mathbf{W}_{lin} \in \mathbb{R}^{1 \times D}$ represent learnable weights, b_{exp} and b_{lin} are biases, Mean denotes the mean fusion, $\hat{y}_{exp}, \hat{y}_{lin}, \hat{y}$ represent the prediction results of ECN, LCN, and FCN, respectively, and L denotes the last number of layers.

5.1.5 **Tri-BCE Loss**. In most CTR prediction models [22, 39, 43], the loss is typically computed solely based on the final prediction $\hat{y}$, overlooking the distinct supervision signals required by individual sub-networks. To address this, we propose Tri-BCE, which provides tailored supervision signals for different sub-networks. The calculation process and balancing method of the multi-loss are illustrated in Figure 7. We use the widely adopted binary cross-entropy (BCE) loss [22, 55] (i.e., Logloss) as both the primary and auxiliary loss for FCN:

$$\mathcal{L} = -\frac{1}{N} \sum_{i=1}^{N} (y_i \log(\hat{y}_i) + (1 - y_i) \log(1 - \hat{y}_i)),$$

$$\mathcal{L}_{exp} = -\frac{1}{N} \sum_{i=1}^{N} (y_i \log(\hat{y}_{exp,i}) + (1 - y_i) \log(1 - \hat{y}_{exp,i})), \quad (10)$$

$$\mathcal{L}_{lin} = -\frac{1}{N} \sum_{i=1}^{N} (y_i \log(\hat{y}_{lin,i}) + (1 - y_i) \log(1 - \hat{y}_{lin,i})),$$

where y denotes the true labels, N denotes the batch size, $\mathcal{L}_{exp}$

---

[3]Other advanced ensemble methods, such as DHEN [50] and HMoE [24], can also be applied here.
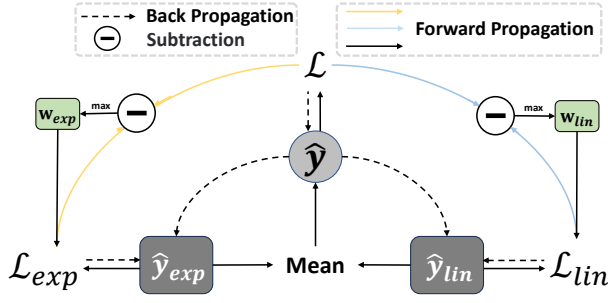
Figure 7: The workflow for the Tri-BCE loss.

and $\mathcal{L}_{lin}$ represent the auxiliary losses for the prediction results of ECN and LCN, respectively, and $\mathcal{L}$ represents the primary loss. To provide each sub-network with suitable supervision signals, we assign them adaptive weights, $\mathbf{w}_{exp} = \max(0, \mathcal{L}_{exp} - \mathcal{L})$ and $\mathbf{w}_{lin} = \max(0, \mathcal{L}_{lin} - \mathcal{L})$, and jointly train them to achieve Tri-BCE:

$$\mathcal{L}_{\text{Tri}} = \mathcal{L} + \mathbf{w}_{exp} \cdot \mathcal{L}_{exp} + \mathbf{w}_{lin} \cdot \mathcal{L}_{lin}, \quad (11)$$

as demonstrated by [16], providing a single supervision signal to sub-networks is often suboptimal. Our proposed Tri-BCE loss helps sub-networks learn better parameters by providing adaptive weights that change throughout the learning process. Theoretically, we can derive the gradients obtained by $\hat{y}_{exp}$:

$$
\begin{aligned}
\nabla_{(\hat{y}_{exp}^+)} \mathcal{L}_{\text{Tri}} &= -\frac{1}{N} \cdot \frac{\partial \left(\log \hat{y}^+ + \mathbf{w}_{exp} \log \hat{y}_{exp}^+ \right)}{\partial \hat{y}_{exp}^+} \\
&= -\frac{1}{N} \left(\frac{1}{2\hat{y}^+} + \frac{\mathbf{w}_{exp}}{\hat{y}_{exp}^+} \right), \\
\nabla_{(\hat{y}_{exp}^-)} \mathcal{L}_{\text{Tri}} &= -\frac{1}{N} \cdot \frac{\partial \left(\log(1 - \hat{y}^-) + \mathbf{w}_{exp} \log(1 - \hat{y}_{exp}^-) \right)}{\partial \hat{y}_{exp}^-} \\
&= \frac{1}{N} \left(\frac{1}{2(1 - \hat{y}^-)} + \frac{\mathbf{w}_{exp}}{1 - \hat{y}_{exp}^-} \right),
\end{aligned}
\quad (12)
$$

where $\nabla_{(\hat{y}_{exp}^+)}$ and $\nabla_{(\hat{y}_{exp}^-)}$ represent the gradients received by $\hat{y}_{exp}$ for positive and negative samples, respectively. Similarly, the gradient signals received by $\hat{y}_{lin}$ are consistent with those of $\hat{y}_{exp}$, so we do not elaborate further. It can be observed that $\hat{y}_{exp}$ and $\hat{y}_{lin}$ both have the same gradient terms, $\frac{1}{2\hat{y}^+}$ and $\frac{1}{2(1-\hat{y}^-)}$, indicating that training both sub-networks with a single loss provides identical supervision signals for both, making it difficult for the two sub-networks to learn and specialize in different types of feature interactions. However, our Tri-BCE loss additionally provides dynamically adjusted gradient terms based on $\mathbf{w}_{exp}$ and $\mathbf{w}_{lin}$, ensuring that the sub-networks are directly influenced by the true labels y and adaptively adjust their weights according to the difference between the primary and auxiliary losses.

5.2 Theoretical Analysis

5.2.1 *ECN is superior to LCN*. To further theoretically clarify the differences between ECN and LCN, we rewrite Eq. (8) by following

the aggregation and interaction steps:

$$\mathbf{x}_{2l} = \mathbf{x}_{2l-1} \odot \text{LCA}\left(\mathbf{x}_{2l-1} \right),$$

$$
= \begin{bmatrix}
\mathbf{e}_{(2l-1,1)} \odot \left[c_{(2l-1,1)} \| c'_{(2l-1,1)} \right] \\
\mathbf{e}_{(2l-1,2)} \odot \left[c_{(2l-1,2)} \| c'_{(2l-1,2)} \right] \\
\vdots \\
\mathbf{e}_{(2l-1,f)} \odot \left[c_{(2l-1,f)} \| c'_{(2l-1,f)} \right]
\end{bmatrix}, \quad (13)
$$

where $\mathbf{e}_{(2l-1,i)} \in \mathbb{R}^d$ denote the 2^{l-1}-th order features of the i-th feature field. By analyzing Eqs. (13) and (6), we observe that, when weight matrices are disregarded, the fully expanded recursive formulation of ECN implements a feature interaction process that can be simplified as:

$$
\begin{aligned}
\mathbf{e}_{(2l,i)} &= \mathbf{e}_{(2l-1,i)} \odot \sum_{i=1}^{f} \mathbf{e}_{(2l-1,i)}, \\
&= \mathbf{e}_{(1,i)} \odot \sum_{i=1}^{f} \mathbf{e}_{(1,i)} \odot \cdots \odot \sum_{i=1}^{f} \mathbf{e}_{(2l-2,i)} \odot \sum_{i=1}^{f} \mathbf{e}_{(2l-1,i)}.
\end{aligned}
\quad (14)
$$

Meanwhile, the feature interaction process of LCN, consistent with CrossNetv2, is expressed as:

$$\mathbf{e}_{(l+1,i)} = \mathbf{e}_{(1,i)} \odot \sum_{i=1}^{f} \mathbf{e}_{(l,i)}. \quad (15)$$

Compared to LCN, ECN facilitates a more sophisticated and comprehensive feature interaction. Through multi-layer recursive expansion, ECN captures higher-order feature interactions, significantly enhancing the CrossNet's expressive capacity.

5.2.2 *Complexity Analysis*. To further compare the efficiency of the DCN series models, we discuss and analyze the time complexity of different models. Let W_Ψ denote the predefined number of parameters in the DNN. The definitions of the other variables can be found in the previous sections. For clarity, we further provide a comparison of the magnitudes of different variables in Table 1. We can derive:

Table 1: Comparison of Analytical Time Complexity
$$s \gg |W_\Psi| > D > f \approx d > L$$

Model	Embedding	Implicit interaction	Explicit interaction
DCNv1 [42]	$O(dfs)$	$O(|W_\Psi|)$	$O(2DL)$
DCNv2 [43]	$O(dfs)$	$O(|W_\Psi|)$	$O(D^2L)$
EDCN [2]	$O(dfs)$	$O(D^2L)$	$O(D^2L)$
GDCN [39]	$O(dfs)$	$O(|W_\Psi|)$	$O(2D^2L)$
ECN	$O(dfs)$	-	$O(D^2L/2)$
FCN$_p$ & FCN$_{sp}$	$O(dfs)$	-	$O(D^2L)$

- Except for our proposed ECN and FCN, all other models include implicit interaction to enhance predictive performance, which incurs additional computational costs.
- In terms of explicit interaction, ECN only has a higher time complexity than DCNv1, and the time complexity of GDCN is four times that of ECN.
- Our FCN model uses the Tri-BCE loss function, which theoretically has a time complexity for loss computation three times higher than other models. However, in practical training, due to

Table 2: Dataset statistics

Dataset	#Instances	#Fields	#Features
Avazu	40,428,967	24	3,750,999
Criteo	45,840,617	39	910,747
ML-1M	739,012	7	9,751
KDD12	141,371,038	13	4,668,096
iPinYou	19,495,974	16	665,765
KKBox	7,377,418	13	91,756
Industrial	$\approx$ 10 Billion	$\approx$ 200	\

optimizations in parallel computation, its training cost is comparable to some models already deployed in production environments (e.g. FinalMLP[22], FINAL[55]) and does not reach the theoretical threefold increase. This is validated in Figure 8. Moreover, this design has no impact on the inference speed.

6 Experiments

6.1 Experiment Setup

6.1.1 Datasets. We evaluate FCN on six CTR prediction datasets: Avazu[4] [56], Criteo[5] [56], ML-1M[6] [34], KDD12[7] [34], iPinYou[8] [27], and KKBox[9] [54]. Table 2 provides detailed information about these datasets. A more detailed description of these datasets can be found in the given references and links.

6.1.2 Data Preprocessing. We follow the approach outlined in [56]. For the Avazu dataset, we transform the timestamp field it contains into three new feature fields: hour, weekday, and weekend. For the Criteo and KDD12 dataset, we discretize the numerical feature fields by rounding down each numeric value x to $\lfloor \log^2(x) \rfloor$ if $x > 2$, and $x = 1$ otherwise. We set a threshold to replace infrequent categorical features with a default "OOV" token. We set the threshold to 10 for Criteo, KKBox, and KDD12, 2 for Avazu and iPinYou, and 1 for the small dataset ML-1M. More specific data processing procedures and results can be found in our open-source run logs[??] and configuration files, which we do not elaborate on here.

6.1.3 Evaluation Metrics. To compare the performance, we utilize two commonly used metrics in CTR models: **Logloss**, **AUC** [34, 39, 53]. AUC stands for Area Under the ROC Curve, which measures the probability that a positive instance will be ranked higher than a randomly chosen negative one. A lower Logloss suggests a better capacity for fitting the data.

6.1.4 Baselines. To verify the superiority of ECN and FCN over models that include implicit feature interactions, we further select several representative baselines, such as PNN [26] and Wide & Deep [3] (2016); DeepFM [7] and DCNv1 [42] (2017); xDeepFM (2018) [19]; AutoInt* (2019) [34]; AFN* (2020) [4]; DCNv2 [43] and EDCN [2], MaskNet [45] (2021); EulerNet [36], FinalMLP [22], FINAL [55] (2023), RFM [37] (2024); DLF [41] (2025).

---

[4]https://www.kaggle.com/c/avazu-ctr-prediction
[5]https://www.kaggle.com/c/criteo-display-ad-challenge
[6]https://grouplens.org/datasets/movielens
[7]https://www.kaggle.com/c/kddcup2012-track2
[8]https://contest.ipinyou.com/
[9]https://www.kkbox.com/intl

6.1.5 Implementation Details. We implement all models using PyTorch [25] and refer to existing works [11, 56]. We employ the Adam optimizer [13] to optimize all models, with a default learning rate set to 0.001. For the sake of fair comparison, we set the embedding dimension to 128 for KKBox and 16 for the other datasets [54, 56]. The Dropout rate is determined via grid search over the set {0, 0.1, 0.2, 0.3}. The batch size is set to 4,096 on the ML-1M and iPinYou datasets and 10,000 on the other datasets. During training, we employ a Reduce-LR-on-Plateau scheduler that reduces the learning rate by a factor of 10 when performance stops improving in any given epoch [54, 56]. To prevent overfitting, we employ early stopping with a patience value of 2. The hyperparameters of the baseline model are configured and fine-tuned based on the *optimal values* provided in [11, 54, 56] and their original paper. For datasets not included in open-source baseline libraries [11, 54, 56], we use a DNN architecture with [400,400,400] and apply the same hyperparameter search strategy as described in the original model papers. For models not covered in [11], we use the source code released by the authors. Further details on model hyperparameters and dataset configurations can be found in our running logs[10].

6.2 Overall Performance

To further comprehensively investigate the performance superiority and generalization ability of FCN on various CTR datasets (e.g., large-scale sparse datasets), we select 16 representative baseline models and 6 benchmark datasets. We highlight the performance of ECN and FCN in bold and underline the best baseline performance. Table 3 presents the experimental results, from which we can make the following observations:

- Overall, FCN achieves the best performance across all six datasets, with an average AUC improvement of 0.25% over the strongest baseline model and an average Logloss decrease of 0.19%, both exceeding the statistically significant threshold of *0.1%*. This demonstrates the effectiveness of FCN. Besides, FCN_p and FCN_{sp} exhibit varying performance across different datasets. Therefore, we recommend flexibly adjusting the network architecture based on data distribution.
- The FinalMLP model achieves good performance on the Avazu and Criteo datasets, surpassing most CTR models that combine explicit and implicit feature interactions. This demonstrates the effectiveness of implicit feature interactions. Consequently, most CTR models attempt to integrate DNN into explicit feature interaction models to enhance performance. However, FCN achieves SOTA performance using only explicit feature interactions, indicating the effectiveness and potential of modeling with explicit feature interactions alone.

6.3 In-Depth Study of FCN

6.3.1 Efficiency Comparison. To verify the efficiency of FCN, we fix the optimal hyperparameters of the 25 baseline models and compare their parameter count (rounded to two decimal places) and runtime (averaged over five runs). The experimental results are shown in Figure 8. We can derive:

---

[10]https://github.com/salmon1802/FCN/tree/KDD'26/checkpoints

Table 3: Performance comparison of different deep CTR models. "*": Integrating the original model with DNN networks. Meanwhile, we conduct a two-tailed T-test to assess the statistical significance between our models and the best baseline (★: $p <$ 1e-3). *Abs.Imp* represents the absolute performance improvement of FCN over the strongest baseline. Typically, CTR researchers consider an improvement of *0.001 (0.1%)* in Logloss and AUC to be statistically significant [2, 40, 42, 56].

Models	Avazu		Criteo		ML-1M		KDD12		iPinYou		KKBox	
	Logloss↓	AUC(%)↑	Logloss↓	AUC(%)↑	Logloss↓	AUC(%)↑	Logloss↓	AUC(%)↑	Logloss↓	AUC(%)↑	Logloss↓	AUC(%)↑
DNN [5]	0.3721	79.27	0.4380	81.40	0.3100	90.30	0.1502	80.52	0.005545	78.06	0.4811	85.01
PNN [26]	0.3712	79.44	0.4378	81.42	0.3070	90.42	0.1504	80.47	0.005544	78.13	0.4793	85.15
Wide & Deep [3]	0.3720	79.29	0.4376	81.42	0.3056	90.45	0.1504	80.48	0.005542	78.09	0.4852	85.04
DeepFM [7]	0.3719	79.30	0.4375	81.43	0.3073	90.51	0.1501	80.60	0.005549	77.94	0.4785	85.31
DCNv1 [42]	0.3719	79.31	0.4376	81.44	0.3156	90.38	0.1501	80.59	0.005541	78.13	0.4766	85.31
xDeepFM [19]	0.3718	79.33	0.4376	81.43	0.3054	90.47	0.1501	80.62	0.005534	78.25	0.4772	85.35
AutoInt* [34]	0.3746	79.02	0.4390	81.32	0.3112	90.45	0.1502	80.57	0.005544	78.16	0.4773	85.34
AFN* [4]	0.3726	79.29	0.4384	81.38	0.3048	90.53	0.1499	80.70	0.005539	78.17	0.4842	84.89
DCNv2 [43]	0.3718	79.31	0.4376	81.45	0.3098	90.56	0.1502	80.59	0.005539	78.26	0.4787	85.31
EDCN [2]	0.3716	79.35	0.4378	81.44	0.3073	90.48	0.1501	80.62	0.005573	77.93	0.4952	85.27
MaskNet [45]	0.3711	79.43	0.4387	81.34	0.3080	90.34	0.1498	80.79	0.005556	77.85	0.5003	84.79
EulerNet [36]	0.3723	79.22	0.4379	81.47	0.3050	90.44	0.1498	80.78	0.005540	78.30	0.4922	84.27
FinalMLP [22]	0.3718	79.35	0.4373	81.45	0.3058	90.52	0.1497	80.78	0.005556	78.02	0.4822	85.10
FINAL [55]	0.3712	79.41	0.4371	81.49	0.3035	90.53	0.1498	80.74	0.005540	78.13	0.4800	85.14
RFM [37]	0.3723	79.24	0.4374	81.47	0.3048	90.51	0.1506	80.73	0.005540	78.25	0.4853	84.70
DLF [41]	0.3720	79.31	0.4382	81.40	0.3083	90.52	0.1497	80.81	0.005540	78.09	0.4884	85.07
ECN	0.3698★	79.68★	0.4365★	81.56★	0.3023★	90.67★	0.1496	80.88★	0.005532★	78.50★	0.4756★	85.59★
FCN$_p$	0.3697★	79.66★	0.4361★	81.60★	0.2975★	90.82★	0.1494★	80.99★	0.005534★	78.48★	0.4747★	85.67★
FCN$_{sp}$	0.3693★	79.72★	0.4357★	81.63★	0.3017★	90.67★	0.1494★	80.96★	0.005529★	78.52★	0.4754★	85.74★
Abs.Imp	-0.0018	+0.29	-0.0014	+0.14	-0.0060	+0.26	-0.0003	+0.18	-0.000010	+0.22	-0.0019	+0.39
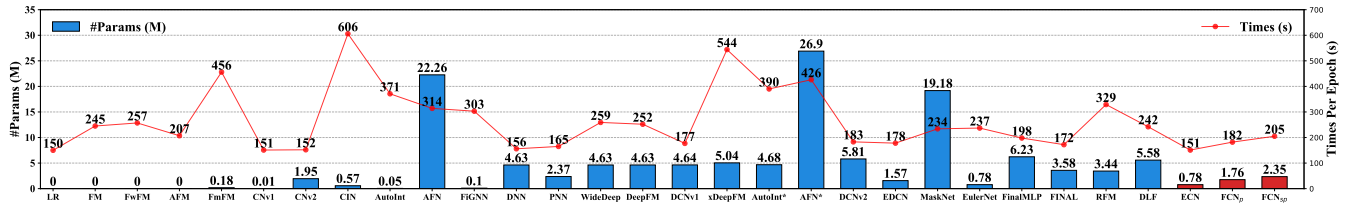
Figure 8: Efficiency comparisons with other models on the Criteo dataset. We only consider non-embedding parameters. We fix the optimal performance hyperparameters for each model and conduct experiments uniformly on one GeForce RTX 4090 GPU.

- Explicit CTR models typically use fewer parameters. For instance, LR, FM, FwFM, and AFM have nearly zero non-embedding parameters, while FmFM, CrossNet, CIN, and AutoInt all require fewer than 1M parameters. Notably, parameter count does not always correlate with time complexity. Although CIN uses only 0.57M parameters, its training time per epoch reaches a maximum of 606 seconds, making it unsuitable for practical production environments. FiGNN and AutoInt face the same issue.

- Compared with models deployed in production environments, such as FinalMLP, FINAL, and DCNv2, our proposed FCN requires fewer parameters while maintaining comparable training cost. With the introduction of the Tri-BCE loss, the training cost of FCN$_{sp}$ increases by only 31 seconds compared to ECN. Besides, the additional computational cost for the loss is incurred solely during training and does not impact inference speed. These results further demonstrate the efficiency of ECN and FCN.

6.3.2 **Ablation Study**. To investigate the impact of each component of FCN$_{sp}$ on its performance, we conduct experiments on several variants using the three datasets where FCN$_{sp}$ achieves SOTA performance.

- **w/o LCN**: FCN$_{sp}$ is constructed solely with ECN, while keeping the architecture and total number of layers unchanged.

Table 4: Ablation study of FCN$_{sp}$.

Model	Criteo		iPinYou		KKBox	
	Logloss ↓	AUC(%) ↑	Logloss ↓	AUC(%) ↑	Logloss ↓	AUC(%) ↑
w/o LCN	0.4362	81.58	0.005534	78.48	0.4758	85.70
w/o ECN	0.4367	81.53	0.005537	78.17	0.4826	85.39
w/o TB	0.4367	81.55	0.005530	78.45	0.4777	85.56
FCN$_{sp}$	0.4357	81.63	0.005529	78.52	0.4754	85.74

- **w/o ECN**: FCN$_{sp}$ is constructed solely with LCN, while keeping the architecture and total number of layers unchanged.
- **w/o TB**: FCN$_{sp}$ with BCE instead of the Tri-BCE.

The results of the ablation experiments are presented in Table 4. We observe that the **w/o LCN** variant results in the smallest performance degradation, while the **w/o ECN** variant leads to the largest performance drop. This indicates that ECN contributes more to the overall model performance than LCN. Meanwhile, the performance decrease of the **w/o LCN** variant also suggests that LCN and ECN serve as complementary interaction methods, employing a two-stream ECN yields suboptimal results. Besides, the variant w/o TB also leads to a certain degree of performance decline, particularly noticeable on KKBox. This further demonstrates the effectiveness of our proposed Tri-BCE.
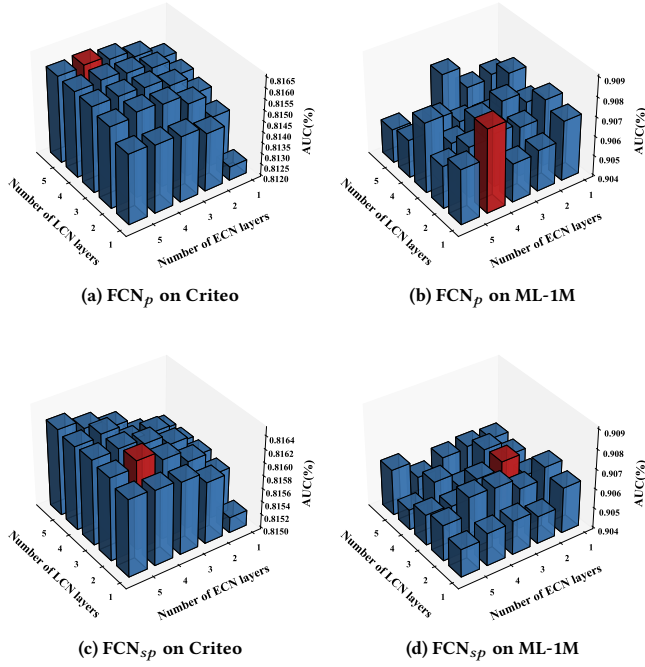
(a) FCN$_p$ on Criteo

(b) FCN$_p$ on ML-1M

(c) FCN$_{sp}$ on Criteo

(d) FCN$_{sp}$ on ML-1M

Figure 9: Performance comparison for different network depths of FCN.

Table 5: Influence of Low-cost Aggregation.

Model	Criteo				KKBox			
	Logloss↓	AUC(%)↑	Params↓	Latency↓	Logloss↓	AUC(%)↑	Params↓	Latency↓
ECN	0.4365	81.56	**0.78M**	**2.85ms**	0.4756	85.59	**5.55M**	**13.54ms**
ECN-full	**0.4363**	**81.57**	1.56M	3.62ms	0.4759	**85.60**	11.08M	17.77ms
FCN$_p$	**0.4361**	**81.60**	**1.76M**	**5.11ms**	**0.4747**	**85.67**	**11.10M**	**27.15ms**
FCN$_p$-full	0.4362	81.59	3.51M	6.54ms	0.4786	85.63	22.16M	34.41ms

6.3.3 *Influence of Network Depths*.
To further investigate the Influence of different neural network depths on the performance of FCN, we conduct experiments on Criteo and ML-1M datasets. From Figure 9, we observe that the optimal layer configurations for FCN$_p$ and FCN$_{sp}$ differ. For instance, on the Criteo dataset, FCN$_p$ achieves optimal performance with a combination of 4 ECN layers and 5 LCN layer, whereas FCN$_{sp}$ performs best with 4 ECN layers and 2 LCN layers.

6.3.4 *Influence of Low-cost Aggregation*.
To investigate the impact of LCA on model performance, we conduct experiments on the Criteo and KKBox datasets. The results are shown in Table 5, where "-full" variant denotes a full-rank network without LCA. We observe that the "-full" variant does not demonstrate significant performance advantages and even suffers from performance degradation in some cases. Meanwhile, the "-full" variant requires twice as many network parameters as LCA and increases inference latency by approximately 23%. These results indicate that LCA effectively reduces model complexity without sacrificing performance.

6.3.5 *The Performance Gap between ECN and LCN*.
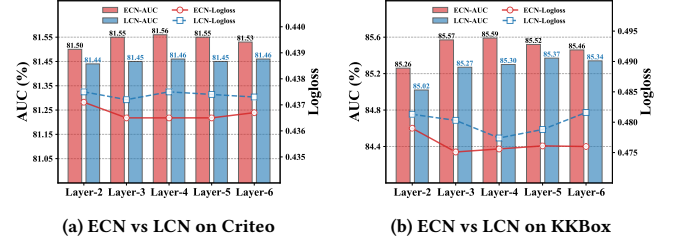To investigate the performance gap between ECN and LCN, we conduct

(a) ECN vs LCN on Criteo

(b) ECN vs LCN on KKBox

Figure 10: Performance comparison of ECN and LCN.

Table 6: Offline results in production settings.

AUC		Day1	Day2	Day3	Day4	Day5	Day6	Day7
Domain 1	DCNv2	**0.8609**	**0.9071**	**0.9209**	**0.9252**	**0.9279**	**0.9250**	**0.9227**
	ECN*	0.8553	0.9054	0.9193	0.9229	0.9272	0.9228	0.9170
Domain 2	DCNv2	0.8414	0.8181	0.8745	0.8454	0.8119	0.8511	0.8391
	ECN*	**0.8647**	**0.8493**	**0.8880**	**0.8921**	**0.8961**	**0.8815**	**0.8773**

the experiments shown in Fig. 10. We observe that as the number of layers increases, ECN consistently outperforms LCN in terms of both AUC and Logloss. This further demonstrates the effectiveness of exponentially growing feature interaction methods.

6.3.6 *Industrial Evaluation*.
To investigate the effectiveness of FCN in industrial-scale recommender systems, we conduct offline evaluations using real production user click logs collected over eight consecutive days (the first seven days serve as the training set, and the last day serves as the validation set). The experimental results are reported in Table 6, which present the prediction performance of seven-day post-click conversion rate (CVR) [21] for clicked samples in two core business domains. Specifically, ECN+ is obtained from DCNv2 by modifying only a single variable in the code, namely replacing the anchor feature from x_1 to x_l. As shown in Table 6, ECN+ performs slightly worse than DCNv2 in Domain 1, while achieving a notable improvement in CVR prediction performance in Domain 2. This indicates that Domain 1 may not require high-order feature interactions, in which case CrossNetv2 suffices, whereas Domain 2 requires higher-order feature interactions to improve model performance.

7 Conclusion

This paper introduced the next generation deep cross network, called FCN, which uses sub-networks LCN and ECN to capture both low-order and high-order feature interactions without relying on the less interpretable DNN. LCN uses a linearly growing interaction method for low-order interactions, while ECN employs an exponentially increasing method for high-order interactions. The low-cost aggregation further improves FCN's computational efficiency. Tri-BCE helped the two sub-networks in FCN obtain more suitable supervision signals for themselves. Comprehensive experiments on six datasets demonstrated the effectiveness and efficiency of FCN.

Acknowledgments

References

[1] Jianxin Chang, Chenbin Zhang, Yiqun Hui, Dewei Leng, Yanan Niu, Yang Song, and Kun Gai. 2023. Pepnet: Parameter and embedding personalized network for infusing with personalized prior information. In *Proceedings of the 29th ACM SIGKDD Conference on Knowledge Discovery and Data Mining*. 3795–3804.

[2] Bo Chen, Yichao Wang, Zhirong Liu, Ruiming Tang, Wei Guo, Hongkun Zheng, Weiwei Yao, Muyu Zhang, and Xiuqiang He. 2021. Enhancing explicit and implicit feature interactions via information sharing for parallel deep CTR models. In *Proceedings of the 30th ACM International Conference on Information & Knowledge Management*. 3757–3766.

[3] Heng-Tze Cheng, Levent Koc, Jeremiah Harmsen, Tal Shaked, Tushar Chandra, Hrishi Aradhye, Glen Anderson, Greg Corrado, Wei Chai, Mustafa Ispir, et al. 2016. Wide & deep learning for recommender systems. In *Proceedings of the 1st Workshop on Deep Learning for Recommender Systems*. 7–10.

[4] Weiyu Cheng, Yanyan Shen, and Linpeng Huang. 2020. Adaptive factorization network: Learning adaptive-order feature interactions. In *Proceedings of the AAAI Conference on Artificial Intelligence*, Vol. 34. 3609–3616.

[5] Paul Covington, Jay Adams, and Emre Sargin. 2016. Deep neural networks for YouTube recommendations. In *Proceedings of the 10th ACM Conference on Recommender Systems*. 191–198.

[6] Ruili Feng, Kecheng Zheng, Yukun Huang, Deli Zhao, Michael Jordan, and Zheng-Jun Zha. 2022. Rank Diminishing in Deep Neural Networks. *Advances in Neural Information Processing Systems* 35 (2022), 33054–33065.

[7] Huifeng Guo, Ruiming Tang, Yunming Ye, Zhenguo Li, and Xiuqiang He. 2017. DeepFM: A Factorization-Machine Based Neural Network for CTR Prediction. In *Proceedings of the 26th International Joint Conference on Artificial Intelligence* (Melbourne, Australia) *(IJCAI'17)*. AAAI Press, 1725–1731.

[8] Boris Hanin. 2018. Which Neural Net Architectures Give Rise to Exploding and Vanishing Gradients? *Advances in Neural Information Processing Systems* 31 (2018).

[9] Tianyu Hua, Wenxiao Wang, Zihui Xue, Sucheng Ren, Yue Wang, and Hang Zhao. 2021. On Feature Decorrelation in Self-supervised Learning. In *Proceedings of the IEEE/CVF international conference on computer vision*. 9598–9608.

[10] Tongwen Huang, Qingyun She, Zhiqiang Wang, and Junlin Zhang. 2020. GateNet: gating-enhanced deep network for click-through rate prediction. *arXiv preprint arXiv:2007.03519* (2020).

[11] Huawei. 2021. An open-source CTR prediction library. https://fuxictr.github.io.

[12] Li Jing, Pascal Vincent, Yann LeCun, and Yuandong Tian. 2022. Understanding Dimensional Collapse in Contrastive Self-supervised Learning. In *International Conference on Learning Representations*. https://openreview.net/forum?id=YevsQ05DEN7

[13] Diederik P Kingma and Jimmy Ba. 2014. Adam: A method for stochastic optimization. *arXiv preprint arXiv:1412.6980* (2014).

[14] Honghao Li, Lei Sang, Yi Zhang, Xuyun Zhang, and Yiwen Zhang. 2023. CETN: Contrast-enhanced Through Network for CTR Prediction. *arXiv preprint arXiv:2312.09715* (2023).

[15] Honghao Li, Lei Sang, Yi Zhang, and Yiwen Zhang. 2024. SimCEN: Simple Contrast-enhanced Network for CTR Prediction. In *Proceedings of the 32th ACM International Conference on Multimedia*.

[16] Honghao Li, Yiwen Zhang, Yi Zhang, Lei Sang, and Yun Yang. 2024. TF4CTR: Twin Focus Framework for CTR Prediction via Adaptive Sample Differentiation. *arXiv preprint arXiv:2405.03167* (2024).

[17] Honghao Li, Yiwen Zhang, Yi Zhang, Lei Sang, and Jieming Zhu. 2025. Revisiting Feature Interactions from the Perspective of Quadratic Neural Networks for Click-through Rate Prediction. In *Proceedings of the 31st ACM SIGKDD Conference on Knowledge Discovery and Data Mining V. 2*. 1365–1375.

[18] Zekun Li, Zeyu Cui, Shu Wu, Xiaoyu Zhang, and Liang Wang. 2019. FiGNN: Modeling feature interactions via graph neural networks for CTR prediction. In *Proceedings of the 28th ACM International Conference on Information and Knowledge Management*. 539–548.

[19] Jianxun Lian, Xiaohuan Zhou, Fuzheng Zhang, Zhongxia Chen, Xing Xie, and Guangzhong Sun. 2018. xDeepFM: Combining explicit and implicit feature interactions for recommender systems. In *Proceedings of the 24th ACM SIGKDD International Conference on Knowledge Discovery & Data Mining*. 1754–1763.

[20] Bin Liu, Chenxu Zhu, Guilin Li, Weinan Zhang, Jincai Lai, Ruiming Tang, Xiuqiang He, Zhenguo Li, and Yong Yu. 2020. AutoFIS: Automatic feature interaction selection in factorization models for click-through rate prediction. In *Proceedings of the 26th ACM SIGKDD International Conference on Knowledge Discovery & Data Mining*. 2636–2645.

[21] Xiao Ma, Liqin Zhao, Guan Huang, Zhi Wang, Zelin Hu, Xiaoqiang Zhu, and Kun Gai. 2018. Entire Space Multi-Task Model: An Effective Approach for Estimating Post-Click Conversion Rate. In *The 41st International ACM SIGIR Conference on Research & Development in Information Retrieval*. 1137–1140.

[22] Kelong Mao, Jieming Zhu, Liangcai Su, Guohao Cai, Yuru Li, and Zhenhua Dong. 2023. FinalMLP: An Enhanced Two-Stream MLP Model for CTR Prediction. *Proceedings of the AAAI Conference on Artificial Intelligence, 37(4), 4552-4560.* (2023).

[23] Junwei Pan, Jian Xu, Alfonso Lobos Ruiz, Wenliang Zhao, Shengjun Pan, Yu Sun, and Quan Lu. 2018. Field-weighted factorization machines for click-through rate prediction in display advertising. In *Proceedings of the 2018 World Wide Web Conference*. 1349–1357.

[24] Junwei Pan, Wei Xue, Ximei Wang, Haibin Yu, Xun Liu, Shijie Quan, Xueming Qiu, Dapeng Liu, Lei Xiao, and Jie Jiang. 2024. Ads Recommendation in A Collapsed and Entangled World. In *Proceedings of the 30th ACM SIGKDD Conference on Knowledge Discovery and Data Mining*. 5566–5577.

[25] Adam Paszke, Sam Gross, Francisco Massa, Adam Lerer, James Bradbury, Gregory Chanan, Trevor Killeen, Zeming Lin, Natalia Gimelshein, Luca Antiga, et al. 2019. PyTorch: An imperative style, high-performance deep learning library. *Advances in Neural Information Processing Systems* 32 (2019).

[26] Yanru Qu, Han Cai, Kan Ren, Weinan Zhang, Yong Yu, Ying Wen, and Jun Wang. 2016. Product-based neural networks for user response prediction. In *2016 IEEE 16th International Conference on Data Mining (ICDM)*. IEEE, 1149–1154.

[27] Yanru Qu, Bohui Fang, Weinan Zhang, Ruiming Tang, Minzhe Niu, Huifeng Guo, Yong Yu, and Xiuqiang He. 2018. Product-based neural networks for user response prediction over multi-field categorical data. *ACM Transactions on Information Systems (TOIS)* 37, 1 (2018), 1–35.

[28] Steffen Rendle. 2010. Factorization Machines. In *2010 IEEE International Conference on Data Mining*. IEEE, 995–1000.

[29] Steffen Rendle, Walid Krichene, Li Zhang, and John Anderson. 2020. Neural collaborative filtering vs. matrix factorization revisited. In *Proceedings of the 14th ACM Conference on Recommender Systems*. 240–248.

[30] Matthew Richardson, Ewa Dominowska, and Robert Ragno. 2007. Predicting clicks: estimating the click-through rate for new ads. In *Proceedings of the 16th International Conference on World Wide Web*. 521–530.

[31] Lei Sang, Honghao Li, Yiwen Zhang, Yi Zhang, and Yun Yang. 2024. AdaGIN: Adaptive Graph Interaction Network for Click-Through Rate Prediction. *ACM Transactions on Information Systems* (2024).

[32] Yunxiao Shi, Wujiang Xu, Zhang Zeqi, Xing Zi, Qiang Wu, and Min Xu. 2025. PersonaX: A Recommendation Agent-Oriented User Modeling Framework for Long Behavior Sequence. In *Findings of the Association for Computational Linguistics: ACL 2025*, Wanxiang Che, Joyce Nabende, Ekaterina Shutova, and Mohammad Taher Pilehvar (Eds.). Association for Computational Linguistics, Vienna, Austria, 5764–5787. doi:10.18653/v1/2025.findings-acl.300

[33] Yunxiao Shi, Shuo Yang, Haimin Zhang, Li Wang, Yongze Wang, Qiang Wu, and Min Xu. 2025. MEGG: Replay via Maximally Extreme GGscore in Incremental Learning for Neural Recommendation Models. *arXiv preprint arXiv:2509.07319* (2025).

[34] Weiping Song, Chence Shi, Zhiping Xiao, Zhijian Duan, Yewen Xu, Ming Zhang, and Jian Tang. 2019. AutoInt: Automatic feature interaction learning via self-attentive neural networks. In *Proceedings of the 28th ACM International Conference on Information and Knowledge Management*. 1161–1170.

[35] Yang Sun, Junwei Pan, Alex Zhang, and Aaron Flores. 2021. FM2: Field-matrixed factorization machines for recommender systems. In *Proceedings of the Web Conference 2021*. 2828–2837.

[36] Zhen Tian, Ting Bai, Wayne Xin Zhao, Ji-Rong Wen, and Zhao Cao. 2023. EulerNet: Adaptive Feature Interaction Learning via Euler's Formula for CTR Prediction. In *Proceedings of the 46th International ACM SIGIR Conference on Research and Development in Information Retrieval*. 1376–1385.

[37] Zhen Tian, Yuhong Shi, Xiangkun Wu, Wayne Xin Zhao, and Ji-Rong Wen. 2024. Rotative Factorization Machines. In *Proceedings of the 30th ACM SIGKDD Conference on Knowledge Discovery and Data Mining*. 2912–2923.

[38] Michael E Wall, Andreas Rechtsteiner, and Luis M Rocha. 2003. Singular Value Decomposition and Principal Component Analysis. In *A practical approach to microarray data analysis*. Springer, 91–109.

[39] Fangye Wang, Hansu Gu, Dongsheng Li, Tun Lu, Peng Zhang, and Ning Gu. 2023. Towards Deeper, Lighter and Interpretable Cross Network for CTR Prediction. In *Proceedings of the 32nd ACM International Conference on Information and Knowledge Management*. 2523–2533.

[40] Fangye Wang, Yingxu Wang, Dongsheng Li, Hansu Gu, Tun Lu, Peng Zhang, and Ning Gu. 2023. CL4CTR: A Contrastive Learning Framework for CTR Prediction. In *Proceedings of the Sixteenth ACM International Conference on Web Search and Data Mining*. 805–813.

[41] Kefan Wang, Hao Wang, Wei Guo, Yong Liu, Jianghao Lin, Defu Lian, and Enhong Chen. 2025. DLF: Enhancing Explicit-Implicit Interaction via Dynamic Low-Order-Aware Fusion for CTR Prediction. *arXiv preprint arXiv:2505.19182* (2025).

[42] Ruoxi Wang, Bin Fu, Gang Fu, and Mingliang Wang. 2017. Deep & cross network for ad click predictions. In *Proceedings of the ADKDD'17*. 1–7.

[43] Ruoxi Wang, Rakesh Shivanna, Derek Cheng, Sagar Jain, Dong Lin, Lichan Hong, and Ed Chi. 2021. DCNv2: Improved deep & cross network and practical lessons for web-scale learning to rank systems. In *Proceedings of the Web Conference 2021*. 1785–1797.

[44] Xianquan Wang, Zhaocheng Du, Jieming Zhu, Chuhan Wu, Qinglin Jia, and Zhenhua Dong. 2025. TayFCS: Towards Light Feature Combination Selection for Deep Recommender Systems. In *Proceedings of the 31st ACM SIGKDD Conference on Knowledge Discovery and Data Mining V. 2*. 5007–5017.

[45] Zhiqiang Wang, Qingyun She, and Junlin Zhang. 2021. MaskNet: Introducing feature-wise multiplication to CTR ranking models by instance-guided mask. *arXiv preprint arXiv:2102.07619* (2021).

[46] Yu Xia, Rui Zhong, Hao Gu, Wei Yang, Chi Lu, Peng Jiang, and Kun Gai. 2025. Hierarchical Tree Search-based User Lifelong Behavior Modeling on Large Language Model. In *Proceedings of the 48th International ACM SIGIR Conference on Research and Development in Information Retrieval*. 1758–1767.

[47] Yu Xia, Rui Zhong, Zeyu Song, Wei Yang, Junchen Wan, Qingpeng Cai, Chi Lu, and Peng Jiang. 2025. TrackRec: Iterative Alternating Feedback with Chain-of-Thought via Preference Alignment for Recommendation. *arXiv preprint arXiv:2508.15388* (2025).

[48] Jun Xiao, Hao Ye, Xiangnan He, Hanwang Zhang, Fei Wu, and Tat-Seng Chua. 2017. Attentional factorization machines: learning the weight of feature interactions via attention networks. In *Proceedings of the 26th International Joint Conference on Artificial Intelligence*. 3119–3125.

[49] Runlong Yu, Yuyang Ye, Qi Liu, Zihan Wang, Chunfeng Yang, Yucheng Hu, and Enhong Chen. 2021. Xcrossnet: Feature structure-oriented learning for click-through rate prediction. In *Pacific-Asia Conference on Knowledge Discovery and Data Mining*. Springer, 436–447.

[50] Buyun Zhang, Liang Luo, Xi Liu, Jay Li, Zeliang Chen, Weilin Zhang, Xiaohan Wei, Yuchen Hao, Michael Tsang, Wenjun Wang, et al. 2022. DHEN: A Deep and Hierarchical Ensemble Network for Large-scale Click-through Rate Prediction. *arXiv preprint arXiv:2203.11014* (2022).

[51] Kexin Zhang, Fuyuan Lyu, Xing Tang, Dugang Liu, Chen Ma, Kaize Ding, Xiuqiang He, and Xue Liu. 2025. Fusion Matters: Learning Fusion in Deep Click-through Rate Prediction Models. In *Proceedings of the Eighteenth ACM International Conference on Web Search and Data Mining (WSDM '25)*. 744–753.

[52] Guorui Zhou, Xiaoqiang Zhu, Chenru Song, Ying Fan, Han Zhu, Xiao Ma, Yanghui Yan, Junqi Jin, Han Li, and Kun Gai. 2018. Deep interest network for click-through rate prediction. In *Proceedings of the 24th ACM SIGKDD International Conference on Knowledge Discovery & Data Mining*. 1059–1068.

[53] Chenxu Zhu, Peng Du, Weinan Zhang, Yong Yu, and Yang Cao. 2022. Combo-fashion: Fashion clothes matching CTR prediction with item history. In *Proceedings of the 28th ACM SIGKDD Conference on Knowledge Discovery and Data Mining*. 4621–4629.

[54] Jieming Zhu, Quanyu Dai, Liangcai Su, Rong Ma, Jinyang Liu, Guohao Cai, Xi Xiao, and Rui Zhang. 2022. Bars: Towards open benchmarking for recommender systems. In *Proceedings of the 45th International ACM SIGIR Conference on Research and Development in Information Retrieval*. 2912–2923.

[55] Jieming Zhu, Qinglin Jia, Guohao Cai, Quanyu Dai, Jingjie Li, Zhenhua Dong, Ruiming Tang, and Rui Zhang. 2023. FINAL: Factorized interaction layer for CTR prediction. In *Proceedings of the 46th International ACM SIGIR Conference on Research and Development in Information Retrieval*. 2006–2010.

[56] Jieming Zhu, Jinyang Liu, Shuai Yang, Qi Zhang, and Xiuqiang He. 2021. Open benchmarking for click-through rate prediction. In *Proceedings of the 30th ACM International Conference on Information & Knowledge Management*. 2759–2769.